

NMR Measurements of Self-Diffusion in Lithium-Ammonia and Sodium-Ammonia Solutions*

A. N. Garroway[†] and R. M. Cotts

Laboratory of Atomic and Solid State Physics, Cornell University, Ithaca, New York 14850

(Received 11 September 1972)

Self-diffusion coefficients of ^7Li , ^{23}Na , and ^1H have been measured in 1–20-MPM (100 \times moles metal/total of moles metal and moles ammonia) solutions of lithium ammonia at 223 and 233 K and in 2–15.5-MPM solutions of sodium ammonia at 233 K by the NMR spin-echo pulsed-magnetic-field-gradient technique. In addition, the temperature dependences of the self-diffusion coefficients were measured for seven representative concentrations of lithium ammonia below 240 K. The data indicate that the lithium and sodium ions are solvated by four ammonia molecules over the time scale of molecular diffusion. The concentration dependence of the self-diffusion coefficients of the metal-ion complexes and of the free-ammonia molecules is found to be consistent, evaluated by the Stokes–Einstein relation, with the available viscosity data. The melting-point self-diffusion coefficient and the temperature dependence of 20-MPM lithium ammonia are fitted to the Ascarello–Paskin and Cohen–Turnbull diffusion models for a reasonable choice of packing fraction.

I. INTRODUCTION

Metal-ammonia solutions exhibit a wide range of physical behavior^{1–3}: As the metal concentration is increased, they pass from an ideal electrolyte through a nonmetal-metal transition and finally become a rather good metal at the highest concentration. Schematic phase diagrams of lithium-ammonia and sodium-ammonia solutions, two of the more thoroughly studied systems, are shown in Fig. 1. The lithium-ammonia solution saturates at approximately 20 MPM, while the saturation concentration for sodium-ammonia solution is about 15.5 MPM near 240 K. [All concentrations will be expressed as $\text{MPM} = 100\% \times \text{moles metal} / (\text{moles metal} + \text{moles ammonia})$.]

In the metallic regime (above 8 MPM) one of the most striking characteristics of metal-ammonia solutions is the rapid increase of electrical conductivity^{4,5} with increasing metal concentration. On increasing from 8 to 20 MPM, the electrical conductivity of the lithium-ammonia solution increases by a factor of 10 and reaches a value of $15 \times 10^3 (\Omega \text{ cm})^{-1}$, a value comparable to that of liquid mercury.

Ashcroft and Russakoff⁶ have successfully explained this concentration dependence by employing a model in which the lithium ions are solvated by λ -ammonia molecules; they chose $\lambda = 4$. They concluded that the $\text{Li}(\text{NH}_3)_4^+$ complex is a rather weak scatterer of electrons, whereas the free-ammonia molecules are strong scatterers. As the lithium concentration is increased above 8 MPM, the number of free-ammonia molecules is rapidly decreased, and it is primarily this depletion which accounts for the strong concentration dependence. This solvation model has also been applied^{7,8} to the analysis of the concentration dependence of the compressibility of lithium-, sodium-, potassium-,

cesium-, and calcium-ammonia solutions.

There is as yet no direct evidence for the existence of the $\text{Li}(\text{NH}_3)_4^+$ complex in the liquid phase. However, the compound lithium tetramine does exist⁹ below 89 K and such solvation might be expected to persist at higher temperatures and perhaps at lower concentrations. If the lithium ion were indeed solvated by four ammonia molecules and if the complex $\text{Li}(\text{NH}_3)_4^+$ diffuses as an entity, then in the saturated solution (20 MPM) the self-diffusion coefficients of the lithium and ammonia should be equal. Furthermore, if this solvation persists in concentrations below 20 MPM, then it would be expected that the larger, more massive $\text{Li}(\text{NH}_3)_4^+$ species should diffuse more slowly than the free-ammonia molecules. Conversely, if the lithium ion were not solvated, then the lithium ion should be more mobile than the ammonia molecules. The self-diffusion coefficients of the ^7Li and of the ammonia protons may be measured independently in the lithium-ammonia solution by the nuclear-magnetic-resonance (NMR) spin-echo pulsed-field-gradient technique as a test of the solvation hypothesis.

Although the sodium-ammonia solution is quite similar to lithium ammonia, no compound of sodium ammonia is known to exist. Measurements of the self-diffusion coefficients of the ^{23}Na and the ammonia protons in sodium ammonia also provide a test of the solvation hypothesis and allow comparison with the behavior of lithium ammonia.

Diffusion measurements in metal-ammonia solutions are of interest for other reasons. Not only is the conductivity of the saturated lithium-ammonia solution comparable to the conductivity of other liquid metals, but the Hall coefficient, thermopower, and Knight shifts are characteristic¹ of liquid metals. If the concentrated lithium-am-

monia solution behaves as a simple metal, then it may provide a test of molecular transport theories in a significantly lower-temperature regime than more common liquid metals: In 20-MPM lithium ammonia diffusion may be studied over a factor of 3 in absolute temperature at pressures well below 1 atm. Second, the mechanical properties of the metal-ammonia solutions change markedly with concentration. On going from pure ammonia to saturated lithium ammonia the density of the solution decreases by 30%. The viscosity¹⁰ decreases by almost 50% from its value for pure ammonia on the addition of 15.4 MPM of lithium. Also, the compressibility¹¹ of 20-MPM lithium ammonia is about twice as large as in pure ammonia. It would then be expected that the self-diffusion coefficients should show a strong concentration dependence and might corroborate explanations which have evolved for the density, viscosity, and compressibility results.

For these motivations diffusion measurements were performed in 1–20-MPM lithium-ammonia and 2–15.5-MPM sodium-ammonia solutions. (Signal-to-noise problems precluded diffusion measurements on the metal nuclei at concentrations much below 1 MPM.)

II. EXPERIMENTAL TECHNIQUE

Pulsed-Field-Gradient Spin-Echo Method

In its simplest form the NMR spin-echo method for measuring self-diffusion coefficients employs a $\frac{1}{2}\pi$ rf pulse followed after a time τ by a π pulse. A spin echo appears at 2τ provided that 2τ is not much longer than the homogeneous T_2 of the nuclear system. If a magnetic gradient is applied after the $\frac{1}{2}\pi$ and π pulses, then a particular spin will constructively interfere with the echo at 2τ provided that the phase gained by precession in the local static magnetic field seen by the spin is equal in the intervals $(0, \tau)$ and $(\tau, 2\tau)$. If the magnetic histories are unequal for many spins, owing to diffusion along the magnetic gradient, then the echo amplitude will be reduced from its value in the absence of diffusion. While diffusion may be measured in a steady (dc) gradient, it may be advantageous to apply a pulsed gradient after the $\frac{1}{2}\pi$ pulse and then an identical pulsed gradient after the π pulse. For a $\frac{1}{2}\pi - \tau - \pi$ sequence the attenuation of the spin echo for pulsed gradients of amplitude G and duration δ , separated by a time τ and delayed from the $\frac{1}{2}\pi$ pulse by t_1 , is¹²

$$M(2\tau) = M'_0 \exp \left\{ - (2\tau/T_2) - [\gamma^2 D G^2 \delta^2 (\tau - \frac{1}{3}\delta) - \frac{2}{3} \gamma^2 D g^2 \tau^3 - 2\gamma^2 D \delta \vec{g} \cdot \vec{G} (\tau^2 - t_1^2 - \delta t_1 - \frac{1}{3}\delta^2)] \right\}, \quad (1)$$

where M'_0 represents the equilibrium magnetization, T_2 the homogeneous transverse relaxation time, γ the nuclear gyromagnetic ratio, D the self-dif-

fusion coefficient, and g the background gradient of the laboratory magnet.

For the large pulsed gradients used in these measurements, the background term (in g^2) and the cross term (in $\vec{G} \cdot \vec{g}$) are small compared to the first term and may be ignored. To avoid mea-

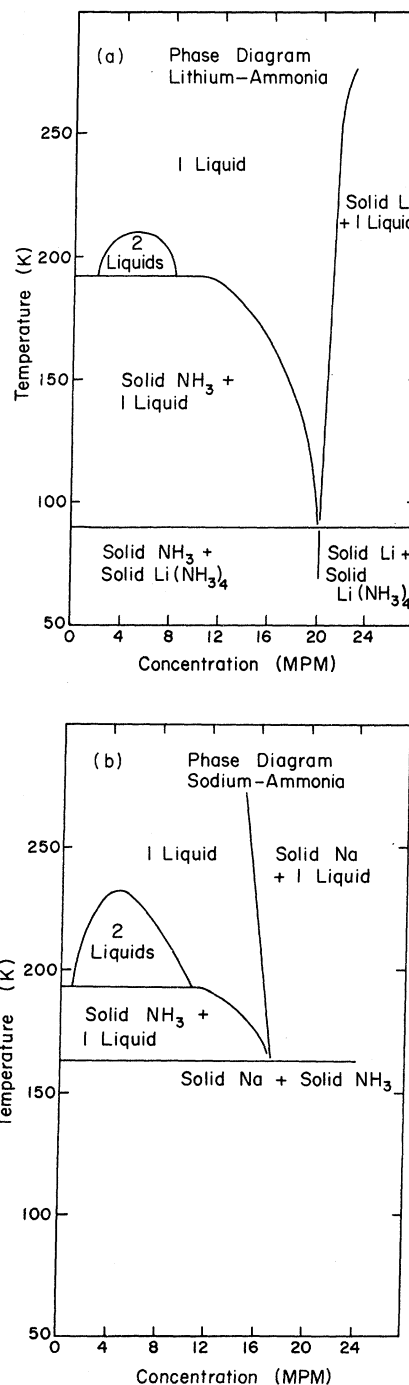


FIG. 1. Phase diagram of (a) lithium ammonia and (b) sodium ammonia adapted from Ref. 2.

suring T_2 , all data were taken for a fixed τ . Corrected¹³ for the finite rise (t_r) and fall (t_f) times of the gradient pulses, Eq. (1) becomes

$$M(2\tau) = M_0 \exp\left\{-\gamma^2 D G^2 \delta^2 \left[\tau - \frac{1}{3} \delta + A(2\tau/\delta - 1)\right]\right\}, \quad (2)$$

where $A = t_r - t_f$ and $M_0 = M'_0 e^{-2\tau/T_2}$. The echo signal was recorded for 8–15 values of (G, δ) and the echo-amplitude data, weighted by the signal-to-noise ratio of the averaged signal, were then computer fit via a least-squares routine to determine the self-diffusion coefficient D .

Sample Geometry

In the concentrated (above 8 MPM) metal-ammonia solutions, an applied rf field induces eddy currents which attenuate and phase shift the applied fields over a distance of the skin depth. For the 20-MPM lithium-ammonia solution this skin depth is about 95μ at 18.5 MHz, the nuclear Larmor frequency selected for the lithium-ammonia diffusion measurements. Thus for a cylindrical sample of radius much greater than 95μ , the magnetic resonance is restricted to a thin annulus at the surface of the liquid and the effective NMR filling factor is significantly reduced, lowering the signal-to-noise ratio from its value in an insulating sample.

Unfortunately, the usual technique of preparing an electrically isolated dispersion of particles smaller than the skin depth is inapplicable for metal-ammonia solutions because of the chemical instability of these solutions in the presence of foreign material. All experiments were therefore performed in "bulk" cylindrical samples, 6-mm-o.d. Pyrex tubes of 1-mm wall thickness filled about 2.5 cm with solution. The problem of measuring self-diffusion coefficients in conducting liquids is treated in the Appendix, which indicates that the analysis [Eq. (2)] of the pulsed-field-gradient spin-echo technique may be applied directly to conducting liquids.

Sample Preparation

Matheson (UHP) ammonia, scrubbed of water in a sodium-ammonia solution, was distilled onto the alkali metals which had been cut and weighed in a helium-filled dry box. The gaseous ammonia was metered out by a mercury manometer and a calibrated volume. The Beatty-Bridgeman¹⁴ equation was used to determine the appropriate pressure of ammonia. The stated compositions of the prepared solutions are accurate to about 1.5%, e.g., 20.0 ± 0.3 MPM.

None of the samples prepared for diffusion measurements showed visible signs of deterioration; these had been stored at 77 K for months and warmed to 90–240 K for hours during measurement. The sodium-ammonia used to dry the am-

monia showed little evolution of hydrogen gas over periods of weeks even though it remained at dry-ice-alcohol bath temperature. As a check on reproducibility, the self-diffusion coefficients of a 15.1-MPM lithium-ammonia solution were remeasured after six months storage and the data agree to within statistical uncertainty. Fifteen samples were destructively analyzed for degradation by measuring the quantity of hydrogen liberated on breaking the sample tubes under vacuum at 77 K. The degradation observed, expressed as the fraction of metal which had been converted into metal amide, ranged from 10^{-4} to 2×10^{-2} , with most samples showing deterioration of about 5×10^{-3} . The few samples older than one year exhibited the greatest degradation.

There is no evidence that the level of sample deterioration affected the diffusion measurement. Certainly the actual metal concentration of the solution was slightly reduced by the deterioration; however, this reduction was always less than or, at worst, equal to the precision to which the samples were originally prepared.

Spectrometer and Gradient Pulser

A medium-power phase-sensitive pulsed NMR spectrometer was used. The spectrometer was modified for use at 18.5 MHz (for lithium ammonia) and 12.5 MHz (sodium ammonia). A slightly unorthodox coil geometry was employed. Since only the tangential component of a time-varying magnetic field penetrates a good electrical conductor, a coaxial geometry allows more field penetration than the standard crossed-coil configuration. A Fabri-Tek model No. 1072 signal averager was used to enhance the signal-to-noise ratio of the detected echo. Extremely-low-level signals were averaged over 64–512 repetitions.

The home-built gradient pulser¹³ produced a maximum gradient of approximately 200 G/cm. The pulsed currents and gradient coil constant were measured independently. As a test of the calibration, the self-diffusion coefficient of partially degassed distilled water was measured to be $(1.90 \pm 0.12) \times 10^{-5} \text{ cm}^2/\text{sec}$ at $(17.7 \pm 0.1)^\circ\text{C}$. Using the measuring temperature dependence¹⁵ of $0.063 \times 10^{-5} \text{ cm}^2/\text{sec K}$, this corresponds to $(2.36 \pm 0.12) \times 10^{-5} \text{ cm}^2/\text{sec}$ at 25°C and compares favorably with other values in the literature.¹⁶

III. RESULTS

Before presenting the diffusion results, it must be established that the self-diffusion coefficient measured for the ammonia protons is actually the self-diffusion coefficient for the ammonia molecules. That is, the distance moved by a proton via interammonia exchange must be small compared to the distance traversed by an ammonia

molecule during its lifetime against intermolecular proton exchange.

In liquid ammonia the scalar coupling of the ^{14}N and proton nuclear spins (I_N and I_P) produces an additional mechanism for longitudinal (T_1) and transverse (T_2) relaxation of the proton¹⁷:

$$\begin{aligned} (T_1^{-1}) &= (T_1^{-1})_{DD} + (T_1^{-1})_{SR} \\ &+ \frac{2}{3} (2\pi J)^2 I_N(I_N + 1) \tau_J / (1 + \omega^2 \tau_J^2), \quad (3) \\ (T_2^{-1}) &= (T_2^{-1})_{DD} + (T_2^{-1})_{SR} \\ &+ \frac{1}{3} (2\pi J)^2 I_N(I_N + 1) [\tau_J + \tau_J / (1 + \omega^2 \tau_J^2)], \end{aligned}$$

where ω is the proton Larmor angular frequency. For liquid ammonia the spin-rotation interactions $(T_1^{-1})_{SR}$ and $(T_2^{-1})_{SR}$ are relatively weak¹⁸ below 250 K and the dipole-dipole rates, $(T_1^{-1})_{DD}$ and $(T_2^{-1})_{DD}$ are equal. The magnitude¹⁹ of the spin-spin coupling J is 46 Hz, and the correlation time of the interaction is τ_J . Mechanisms which modulate the spin-spin interaction are the T_1 relaxation of the ^{14}N spins and intermolecular proton exchange. By Eq. (3), a lower bound of 4×10^{-4} sec for the intermolecular-exchange correlation time is obtained from the proton relaxation times observed in these diffusion measurements and by the assumption that the intermolecular exchange mechanism predominates in the modulation of the spin-spin interaction. Since this correlation time is many orders of magnitude greater than molecular-ammonia jump times, the self-diffusion coefficient measured for the ammonia protons is equal to the coefficient for the ammonia molecules.

Figure 2 shows echo-amplitude data, used in Eq. (2) for the calculation of the self-diffusion coefficients, under the most favorable (2-MPM lithium ammonia) and least favorable (20-MPM lithium ammonia) conditions of the experiment. In the concentrated solution the high electrical conductivity has limited the resonance to a thin annulus at the sample's surface, and the low static susceptibility at this relatively high temperature has further reduced the magnetization available for echo formation. As shown in Fig. 2(a), sufficient signal was available to reduce the echo amplitude by almost 1000 from its value in the absence of a pulsed field gradient; the linearity of the curve shows that the pulsed currents have been measured consistently. Data for the lithium and sodium resonances are similar although the resonances are somewhat weaker than for the protons.

The self-diffusion coefficients of the lithium and ammonia were measured as a function of tem-

perature for the 2.01-, 5.41-, 10.8-, 15.1-, 19.7-, and 20.0-MPM lithium-ammonia samples; the self-diffusion coefficient in pure ammonia was

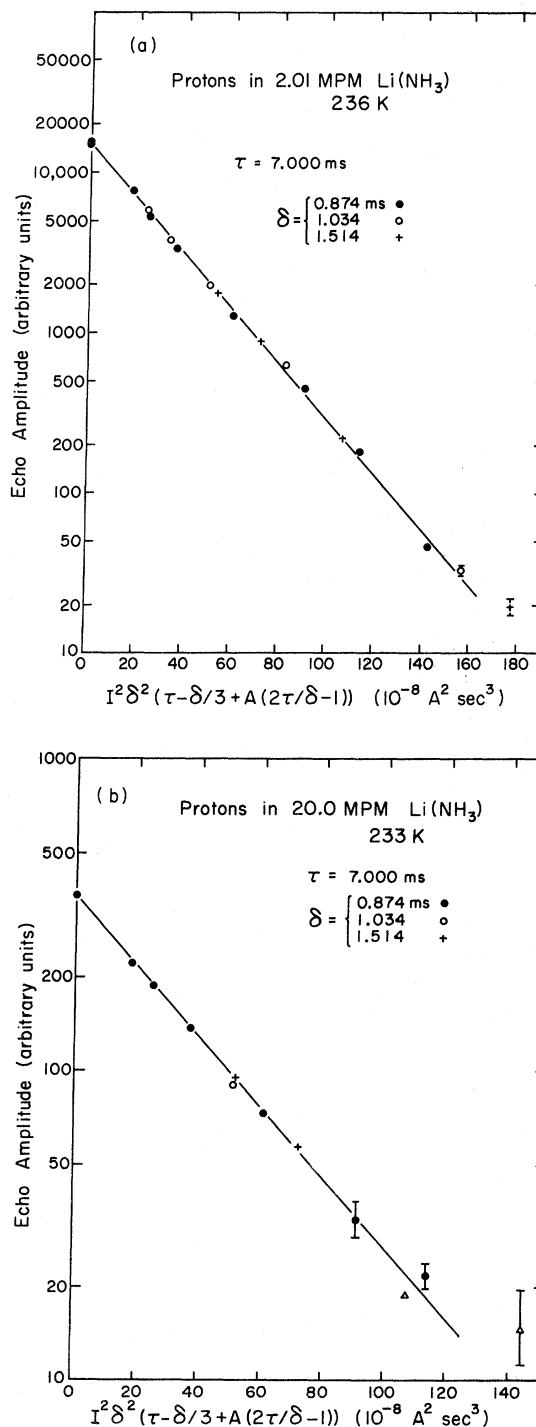


FIG. 2. Proton echo-amplitude data for (a) 2-MPM and (b) 20-MPM lithium ammonia.

also measured. These results are shown in Figs. 3 and 4. Reference to the phase diagrams (Fig. 1) shows that the solutions begin to concentrate by freezing out excess ammonia as the temperature is lowered below the phase boundary. Figures 3(b)–3(e) indicate the change in the self-

diffusion coefficients near the phase boundaries. In particular, below about 160 K in the 15.1-MPM solution, the self-diffusion coefficients of the lithium and ammonia are essentially equal, just as in the 20-MPM sample.

Diffusion measurements were performed for

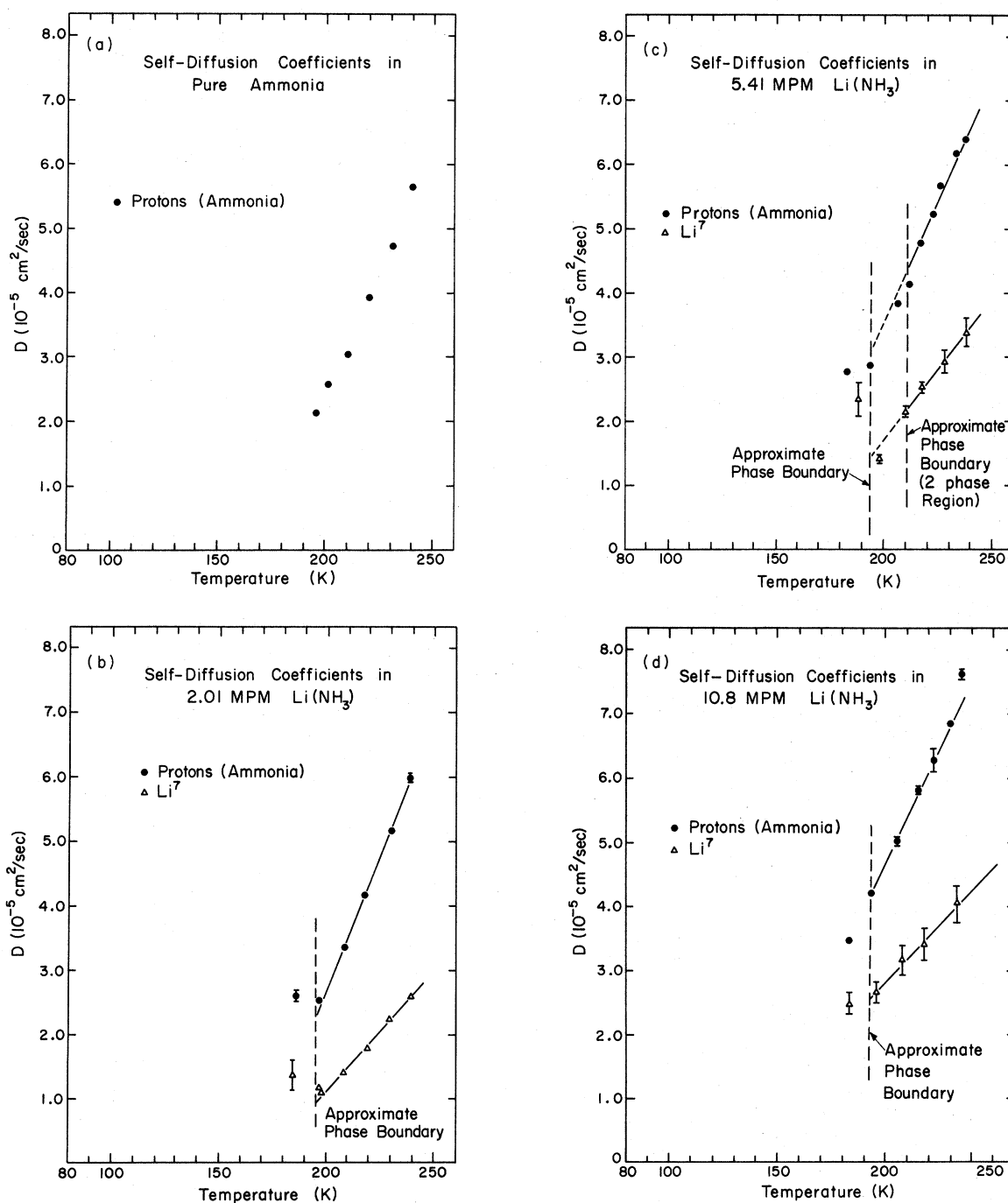


FIG. 3. Self-diffusion coefficients in lithium-ammonia solutions as a function of temperature. The solid curves are drawn for comparison only and have no theoretical significance.

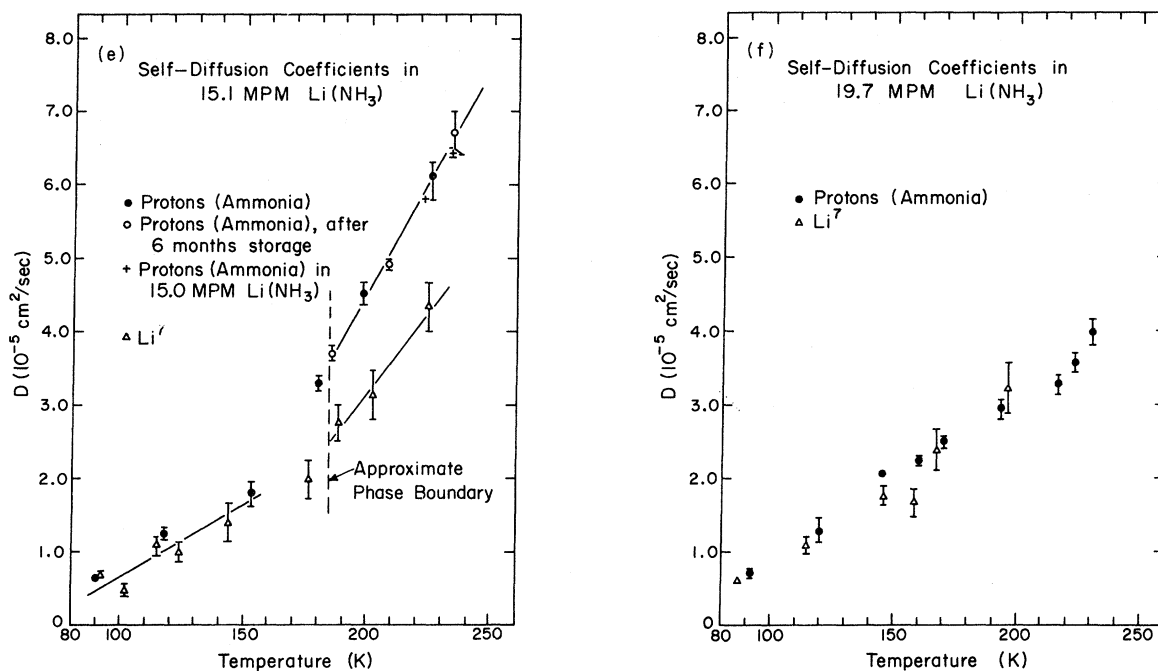


FIG. 3. (Continued)

other concentrations at the isotherms 223 and 233 K, and the data are shown in Fig. 5. Also shown are the results of Figs. 3 and 4 which have been interpolated to 223 and 233 K by an Arrhenius fit; data below the phase boundary were, of course,

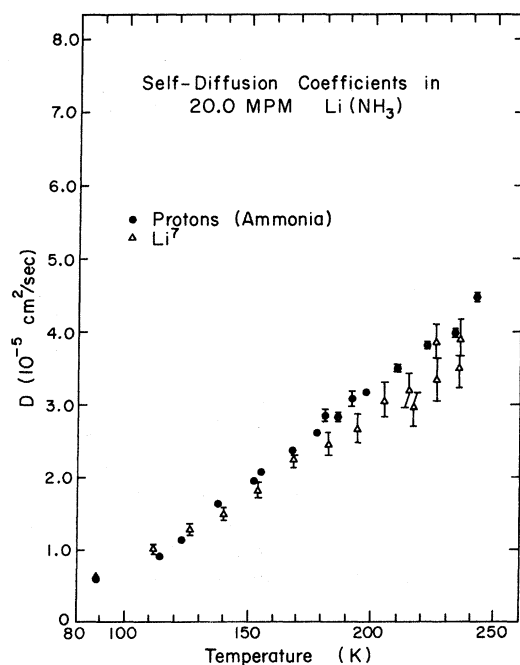


FIG. 4. Self-diffusion coefficients in a 20.0-MPM lithium-ammonia solution as a function of temperature.

excluded from the fit. The results for the 19.7-MPM solution are similar to those for the 20-MPM sample and are omitted from Fig. 5 for clarity. The error bars indicate only the statistical uncertainty of the least-squares fit. All measurements may be systematically in error by 4.5%, since the gradient-coil constant and pulsed currents were measured to 2.1 and 0.15%, respectively.

Figure 5 shows that both the lithium and ammonia self-diffusion coefficients increase with concentration to about 12 MPM. Above 12 MPM the lithium self-diffusion coefficient then levels off or perhaps decreases slightly, while the ammonia coefficient decreases by a factor of 2 until it is essentially equal to the lithium self-diffusion coefficient at 20 MPM. The ammonia self-diffusion coefficient for a 22-MPM sample is plotted at the 22-MPM abscissa. However, since lithium ammonia saturates at about 20 MPM, this sample consists of a saturated lithium-ammonia solution and a small amount of lithium metal, and the measured self-diffusion coefficient is consistent with the result for the 20-MPM solution.

For the sodium-ammonia solution, diffusion data were taken only at 233 K for 2.0-, 5.0-, 8.0-, 12.5-, 14.0-, and 15.5-MPM samples and are displayed in Fig. 6. Comparing Figs. 5 and 6 the concentration dependence and indeed the actual values of the metal and ammonia self-diffusion coefficients are seen to be very similar for both lithium and sodium systems. The equality of the

sodium self-diffusion coefficients in the 15.5- and 17.0-MPM solutions suggests that saturation has occurred at approximately 15.5 MPM at 233 K.

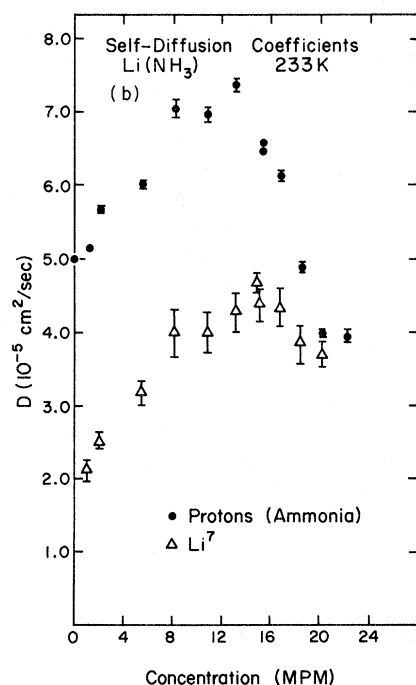
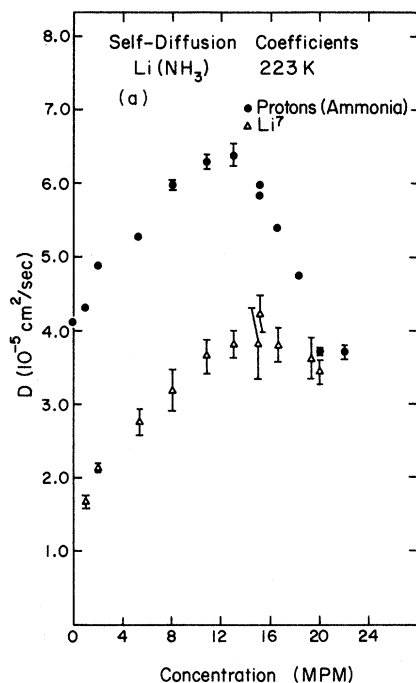


FIG. 5. Self-diffusion coefficients in lithium ammonia as a function of concentration. This figure includes the data of Figs. 3 and 4 as well as data for additional samples.

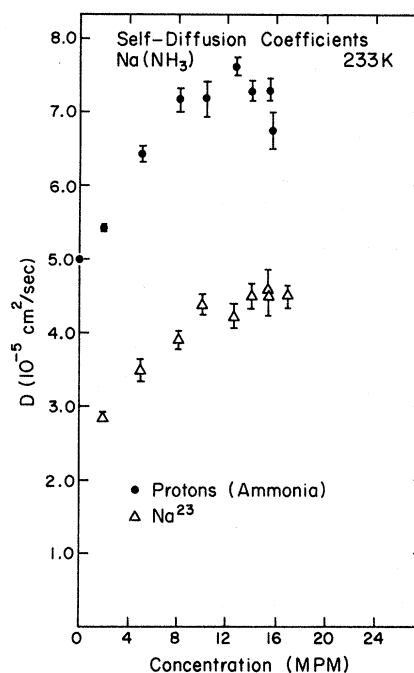


FIG. 6. Self-diffusion coefficients in sodium ammonia as a function of concentration.

IV. DISCUSSION

The elementary Stokes-Einstein theory of diffusion in liquids, while a macroscopic theory, has been applied with some success to molecular fluids and may be used to decide if the metal-ammonia diffusion results are consistent with a solvation model. In the Stokes-Einstein theory particles of radius a are considered to diffuse in a homogeneous fluid of viscosity ν . The self-diffusion coefficient is²⁰

$$D = (1/6\pi a)(kT/\nu), \quad (4)$$

where k is Boltzmann's constant and T is the absolute temperature.

Since the ionic radius²¹ of ${}^7\text{Li}$ (0.60 Å) is much smaller than the ammonia van der Waals radius²¹ (1.54 Å), Eq. (4) predicts that the observed self-diffusion coefficient of the lithium should be much greater than for ammonia. Furthermore, since the viscosities of lithium-ammonia and sodium-ammonia solutions are approximately equal at equivalent concentrations, the expected self-diffusion coefficient of lithium should be greater than that of sodium (ionic radius²¹ 0.95 Å). The diffusion results (Figs. 5 and 6) show that for all concentrations except 20 MPM the ammonia self-diffusion coefficient exceeds that of lithium and further that the sodium and lithium self-diffusion coefficients are essentially equal at equivalent concentrations. Hence the diffusing species do

not appear to be free-metal ions and free-ammonia molecules: The smaller lithium self-diffusion coefficient indicates that the lithium is impeded in its motion.

The lithium-ammonia results may be understood by considering the fluid to be a homogeneous mixture of lithium ions solvated by four ammonia molecules and free-ammonia molecules. The lithium ion is assumed to be solvated during a diffusive step; that is, the cage of four ammonia molecules is dragged along as the lithium changes position. (If the time scale of solvation were shorter, then the lithium ion would appear unsolvated in its diffusional motion, in contradiction to the data of Fig. 5.) For a concentration x , expressed in MPM, the fraction of free-ammonia molecules F_f and the fraction of bound-ammonia F_b molecules is

$$\begin{aligned} F_f &= (100 - 5x)/(100 - x), \\ F_b &= 4x/(100 - x). \end{aligned} \quad (5)$$

If the exchange between the free and bound species were slow compared to the time of the diffusion measurement (7 msec), then two separate diffusion coefficients should be observed and the proton echo should be given by the superposition

$$\begin{aligned} M_0 \{ &F_b \exp[-\gamma^2 D_b G^2 \delta^2 \{\tau - \frac{1}{3} \delta + A(2\tau/\delta - 1)\}] \\ &+ F_f \exp[-\gamma^2 D_f G^2 \delta^2 \{\tau - \frac{1}{3} \delta + A(2\tau/\delta - 1)\}] \}, \end{aligned} \quad (6)$$

where D_b and D_f represent the bound and free self-diffusion coefficients. The Stokes-Einstein relation would predict that $D_f \approx 2D_b$. At 10.8 MPM, 52% of the ammonia is free and the remainder is bound. However, for the 10.8-MPM sample there is no evidence from the echo-amplitude data for the superposition of two exponential functions associated with two values of D . Therefore the exchange of free- and bound-ammonia molecules is rapid on the millisecond time scale, and over this interval a particular ammonia molecule will spend a fraction of time F_b attached to lithium ions and a fraction F_f as a free entity. The measured self-diffusion coefficient then represents the following average:

$$\langle D \rangle = F_b D_b + F_f D_f. \quad (7)$$

Under this four-to-one solvation model, at 20 MPM all the ammonia molecules are associated with lithium complexes and thus the lithium and (averaged) ammonia self-diffusion coefficients should be equal. Figure 4 shows that the coefficients are essentially equal from 90 to 240 K. The slight discrepancy is not understood. If the solvation involves exactly a four-to-one ratio, then the data are consistent with a 19.7-MPM solution. In fact, since the samples were prepared to only 1.5% of their stated composition, the stoichiometry of the 20-MPM sample is 20.0 ± 0.3

MPM. (The fraction of lithium metal which had degraded into lithium amide, measured by the technique outlined in Sec. II, was 3×10^{-3} , too small to account completely for the observed discrepancy.) On the other hand, if the composition were exactly 20.0 MPM, then the effective solvation number is 3.8–3.9. It is possible that the solvation number is temperature dependent. Unfortunately, the scatter of the diffusion data precludes a check for such temperature dependence.

The equality of the self-diffusion coefficients at saturation (20 MPM) is the strongest indication that the lithium ions are solvated by four ammonia molecules. At lower concentrations the solvation number cannot be unambiguously determined, although the ratio of the metal-to-ammonia self-diffusion coefficients definitely implies some solvation.

The sodium-ammonia solution does not reach a concentration at which the sodium and ammonia self-diffusion coefficients are equal and the solvation number cannot be exactly prescribed. Since at 233 K in the 15.5-MPM solution the sodium self-diffusion coefficient is smaller than that of ammonia, the solvation number must be less than $(100 - 15.5)/15.5 = 5.45$. The reassuring similarity of the lithium-ammonia and sodium-ammonia diffusion data suggests that the sodium ion is also solvated by four ammonia molecules.

By assuming that the solvation number is concentration independent, the self-diffusion coefficient of the free-ammonia molecules may be unfolded from the experimental data by Eq. (7); the free-ammonia results so derived are shown in Fig. 7 for lithium ammonia at 223 K and for both lithium ammonia and sodium ammonia at 233 K. Again, the similarity of the data indicates that the solvation numbers are not very different for the two systems.

For both the lithium- and sodium-ammonia solutions, the Stokes-Einstein radii ($a = kT/6\pi D\nu$) may be calculated from the measured self-diffusion coefficients and the viscosity information. Viscosity data are available¹⁰ for lithium ammonia at 233 K and higher temperatures and were extrapolated to 223 K. Sodium-ammonia viscosity data are available²² at 233 K. The calculated radii of the metal complexes and of the free-ammonia molecules are displayed in Fig. 8; error bars represent only the statistical uncertainty in D and do not reflect systematic errors in D or uncertainties in the viscosity data. The calculated radii for the $\text{Li}(\text{NH}_3)_4^+$ and $\text{Na}(\text{NH}_3)_4^+$ complexes are essentially equal and approximately twice as large as the free-ammonia radius. The 20% decrease at about 4 MPM is not understood. McCall and Douglass²³ have noted a similar but not universal decrease for aqueous solutions of electrolytes at molarities of about 2 M.

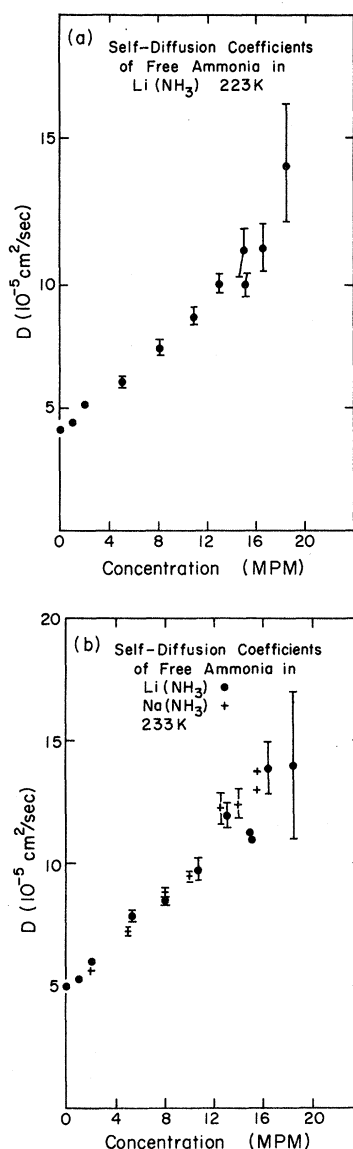


FIG. 7. Self-diffusion coefficients of the free-ammonia molecules in lithium ammonia and sodium ammonia as a function of concentration. A solvation number of four has been assumed for both systems.

To stress the simple Stokes-Einstein relation even further, the temperature dependence of the self-diffusion coefficients and viscosity may be compared provided the characteristic radii are temperature independent. For the limited subset of samples for which temperature dependences were measured, the self-diffusion coefficients of the metal complexes and the free-ammonia molecules were fit to the Arrhenius relation $D = D_0 e^{-E_D/RT}$. The results, shown in Fig. 9, are somewhat imprecise owing to the paucity of data. Viscosity activation energies, derived from a fit to $\nu/T = (\nu/T)_0 e^{E_\nu/RT}$, are also shown. If the Stokes-Ein-

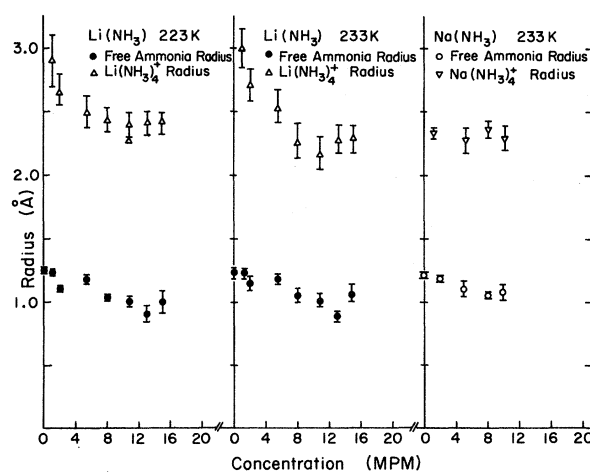


FIG. 8. Stokes-Einstein radii for lithium ammonia and sodium ammonia as a function of concentration. The radii were calculated from the measured self-diffusion coefficients and the available viscosity data.

stein relation is obeyed, then $E_D = E_\nu$. From Fig. 9 the concentration dependences of E_ν and E_D for both free ammonia and the metal complex are similar and numerical agreement is fair.

Unfortunately, viscosity data are not available beyond 15 MPM, where the lithium self-diffusion coefficient shows a leveling off or even a decrease with increasing concentration (Fig. 5). It may be speculated that the viscosity data would also mirror this behavior.

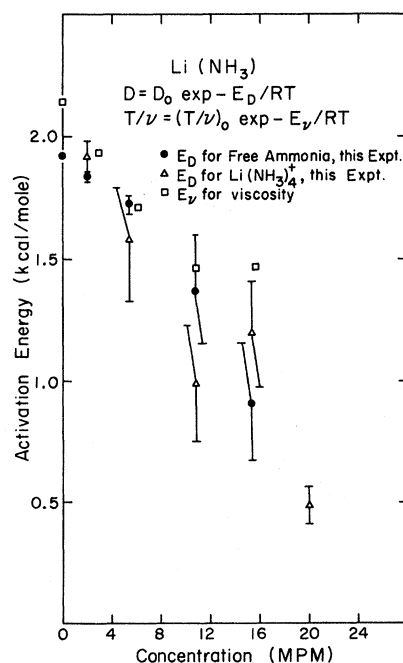


FIG. 9. Activation energies of the self-diffusion coefficients and of viscosity in lithium ammonia.

Saturated Lithium-Ammonia Solution

The equality of the lithium and (averaged) ammonia self-diffusion coefficients suggests the 20-MPM solution may be treated as a single-component fluid. It is therefore appealing to treat the solution in the context of a simple hard-sphere model and to predict the self-diffusion coefficient at melting and its temperature dependence by diffusion models which have been successful for other liquid metals.

The Ascarello-Paskin model for diffusion in a dense gas of hard spheres predicts²⁴

$$D = 0.73 \left(\frac{\eta_m}{\eta} \right) \left(\frac{r}{2} \right) \left(\frac{\pi k T}{m} \right)^{1/2} \frac{1}{z_m (T_m \rho / T \rho_m) - 1}, \quad (8)$$

where η is the packing fraction, r is the hard-sphere radius, m is the mass of the diffusing species, and z is the hard-sphere compressibility. The subscript m denotes the melting-point value. The packing fraction is given by

$$\eta = \frac{4}{3} \pi r^3 \rho, \quad (9)$$

where ρ is the number density of hard spheres. Vadovic and Colver²⁵⁻²⁷ recommend using the Carnahan-Starling expression for z ²⁸:

$$z = (1 + \eta + \eta^2 - \eta^3) / (1 - \eta)^3. \quad (10)$$

Ashcroft and Lekner²⁹ have found that the structure factor of liquid metals may be well approximated by taking $\eta = 0.45$ at melting. The temperature dependence (logarithmic derivative) at melting of the self-diffusion coefficient is calculated to be, for $\eta_m = 0.45$,

$$\left. \frac{T}{D} \frac{dD}{dT} \right|_m = 1.86 + 1.70 \alpha_m T_m, \quad (11)$$

where α_m is the thermal-volume-expansion coefficient at melting and T_m is the melting temperature, 89 K in the case of 20-MPM lithium ammonia. Since $\alpha_m T_m \ll 1$ for normal metals, Eq. (11) predicts that the temperature dependence of the self-diffusion coefficient is essentially equal for all metals, within the confines of this model.

For the 20-MPM solution, extrapolating Lo's density data³⁰ for ρ_m and α_m , Eqs. (8) and (11) predict $D_m = 2.2 \times 10^{-5}$ cm²/sec and $(T/D) (dD/dT)_m = 1.92$. The experimentally determined values are $D_m = (0.59 \pm 0.5) \times 10^{-5}$ cm²/sec and $(T/D) (dD/dT)_m = 1.97 \pm 0.05$. Agreement between the experimental values and the predictions of the Ascarello-Paskin model (for $\eta_m = 0.45$) is poor for D_m and perhaps fortuitous for the temperature dependence.

A value of η_m may be calculated from the hard-sphere model for the isothermal compressibility K_T ³¹:

$$K_T = \frac{v_M}{kT} \frac{(1 - \eta)^4}{(1 + 2\eta)^2}, \quad (12)$$

where v_M is the volume per molecule. While this model ignores the electronic contribution to the

compressibility, it has been employed^{7,8} with some success for concentrated metal-ammonia solutions. Since the isothermal compressibility is approximately equal to the adiabatic compressibility for metals, fitting the adiabatic compressibility obtained from sound-velocity measurement³² near melting to Eq. (12) yields $\eta_m = 0.61$. Using this value of η_m in the Ascarello-Paskin model, $D_m = 0.73 \times 10^{-5}$ cm²/sec and $(T/D) (dD/dT)_m = 1.72$. Thus a somewhat better fit occurs for $\eta_m = 0.61$, a large but not unphysical value.

The diffusion model of Cohen and Turnbull³³ may also be applied. Hard spheres of radius r are considered to move into holes whose size must exceed some critical volume v^* . Fluctuations in the free volume v_f available to each sphere open up holes for a diffusive step. The Cohen-Turnbull result is

$$D = \frac{1}{6} (2r) (kT/m)^{1/2} e^{-\Gamma v^*/v_f}, \quad (13)$$

where Γ is a correction factor of the order of unity for the overlap of the free volume. The temperature dependence is then

$$\frac{T}{D} \frac{dD}{dT} = \frac{1}{2} + \frac{T}{r} \frac{dr}{dT} + \frac{\Gamma v^*}{v_f} \left(\frac{T}{v_f} \right) \frac{dv_f}{dT}. \quad (14)$$

Various forms are available^{33,34} for the functional relation of v_f upon v_M , the mean volume per molecule. In particular, v_f may be related to v_M by the hard-sphere compressibility

$$\frac{v_M}{v_f} \frac{dv_f}{dv_M} = z. \quad (15)$$

Using Eqs. (14), (15), and (10) and setting $\eta_m = 0.45$, the temperature dependence is

$$\left. \frac{T}{D} \frac{dD}{dT} \right|_m = 0.332 + 9.385 \left(\frac{\Gamma v^*}{v_f} \right)_m + 0.215 \alpha_m T_m. \quad (16)$$

The measured value of D_m may be used to determine $(\Gamma v^*/v_f)_m = 2.8$ by Eq. (13) and hence Eq. (16) predicts that $(T/D) (dD/dT)_m = 1.37$, a value lower than the experimental value of 1.97 ± 0.05 . By varying η_m and hence z_m , a fit to both D_m and $(T/D) (dD/dT)_m$ may be forced; the Cohen-Turnbull predictions agree with experiment if η_m is selected to be 0.52.

Both the Ascarello-Paskin and Cohen-Turnbull models require melting-point packing fractions greater than 0.45 to agree with the experimental results. This may indicate that the rather knobby structure of the tetrahedral array of ammonia molecules about the lithium ion impedes diffusion, and hence the effective radius and therefore the packing fraction of the $\text{Li}(\text{NH}_3)_4^+$ complex are increased over the value expected for a more spherical species.

Saxton and Sherby³⁵ have noted that the measured self-diffusion coefficients of pure metals may be fit to the relation $D = D_0 e^{-N T_m / T}$, where N ranges

from 2.5 to 4.0 for different metals. The 20-MPM lithium-ammonia diffusion data give $N = 2.75 \pm 0.05$, where T_m is taken to be 89 K. Thus the temperature dependence of D for the $\text{Li}(\text{NH}_3)_4^+$ complex in 20-MPM lithium ammonia is consistent with those of other liquid metals.

V. CONCLUSIONS

The self-diffusion coefficients of ^7Li and ^1H in lithium ammonia and of ^{23}Na and ^1H in sodium ammonia have been measured in the liquid phase over the range of (1 MPM)—saturation for lithium ammonia and (2 MPM)—saturation for sodium ammonia. In the liquid the lifetime of an ammonia molecule against intermolecular proton exchange is long on the time scale of molecular collisions and the measured self-diffusion coefficient of the proton is equal to that of the ammonia molecule. The observation that the measured ammonia self-diffusion coefficient is greater than the lithium self-diffusion coefficient, except at 20 MPM where they are essentially equal, suggests strongly that the lithium ion is solvated by four ammonia molecules. The similarity of the sodium-ammonia and lithium-ammonia diffusion data indicates that the solvation number is also four in the case of sodium ammonia. Since exchange among free- and bound-ammonia molecules is rapid on the time scale of the experiment, the self-diffusion coefficient represents an average over the two states, and the self-diffusion coefficient of the free-ammonia molecules was unfolded from the experimental diffusion data on the assumption that the solvation number is concentration independent. The Stokes-Einstein radii calculated for the metal complexes and for the free-ammonia molecules from the available viscosity information are essentially concentration independent in both lithium ammonia and sodium ammonia, indicating that the solvation number is not strongly concentration dependent. Fair agreement is obtained for lithium ammonia on comparing the activation energies of the self-diffusion coefficients with those of the Arrhenius fit to T/ν .

Two models of diffusion, the Cohen-Turnbull and Ascarelli-Paskin models, were applied to the 20-MPM lithium-ammonia solution since it may be regarded as a single-component system. Agreement with model predictions is achieved for melting-point packing fractions greater than 0.45.

This work has also demonstrated that NMR spin echoes may be observed in bulk liquid conductors and further that the self-diffusion coefficients may be measured providing the effects of restricted diffusion are not severe.

ACKNOWLEDGMENTS

Professor N. W. Ashcroft had originally suggested that NMR diffusion measurements might

disclose solvation effects in concentrated lithium-ammonia solutions and we have benefited from further discussions with him. This work has also profited from the perspectives of Professor M. J. Sienko.

APPENDIX: DIFFUSION MEASUREMENTS IN CONDUCTING LIQUID

As an rf field penetrates a good electrical conductor, it is attenuated and phase shifted relative to the surface over a characteristic skin depth Δ . For the most conducting solution studied, 20-MPM lithium ammonia, this skin depth is 95μ at 18.5 MHz and in a cylindrical sample the magnetic resonance is essentially restricted to a thin annulus at the surface. This appendix discusses diffusion measurements under these conditions. The formation of a spin echo in a conducting liquid will be first outlined and then the effects of restricted diffusion will be considered.

For a cylindrical sample of radius R with cylinder axis aligned coaxial to a transmitter coil producing a field of $2H_1 \sin \omega t$ at the sample's surface, the field at radius r inside the conductor, in the primed reference frame rotating at the Larmor angular frequency ω , is

$$H_1(r) = H_1 e^{-(R-r)/\Delta} e^{-i(R-r)/\Delta} \quad (17)$$

To consider the formation of a spin echo within a "differential" annulus of radius r and width dr , it is convenient to introduce a doubly primed frame which again rotates with frequency ω but is rotated about the z axis by the angle $\tan^{-1}[(R-r)/\Delta]$ with respect to the primed reference frame. The relation among these reference frames is shown in Fig. 10. If the resonant rf field nutates the nuclear spins at the surface by an angle θ_0 , then for a $\theta_0 - \tau - 2\theta_0$ pulse sequence the amplitude of the echo formed in the annulus is³⁶

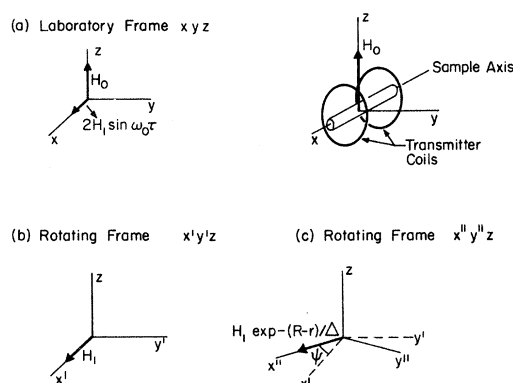


FIG. 10. (a) Laboratory reference frame defined by the orientation of H_0 and the transmitter coil; (b) primed rotating frame; and (c) doubly primed rotating frame.

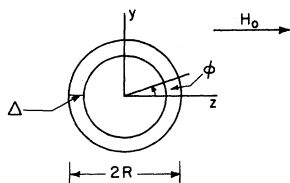


FIG. 11. Differential annulus.

$$dm(r) = dm_0(r) \sin\theta \sin^2\theta e^{-2\pi T_2}, \quad (18)$$

where $dm_0(r)$ represents the equilibrium magnetization in the annulus, and $\theta = \theta_0 e^{-(R-r)/\Delta}$. The echo formed in the annulus appears along the $-y''$ axis at the time 2τ ; that is, the echo is phase shifted by $\tan^{-1}[(R-r)/\Delta]$ relative to the echo formed at the surface. For $\theta_0 = \frac{1}{2}\pi$, the echo formed near the surface is largest; the attenuation of H_1 makes echo formation more inefficient further into the sample.

The signal induced in the receiver coil by the echo formed in each differential annulus is further phase shifted and attenuated by eddy currents produced by the echo. McLachlan³⁷ has calculated the signal induced by the precession of spins subjected to a θ pulse. Applying his results to the case of the spin echo,

$$v(2\tau) \propto (e^{-2\tau/T_2}) \int_0^\infty dm(r) \sin\theta \sin^2\theta \times \cos^2[(R-r)/\Delta] e^{-(R-r)/\Delta}, \quad (19)$$

where R is assumed much greater than Δ .

Now Muller and Bloom³⁸ have shown that the attenuation of an echo due to diffusion in a steady-field magnetic field gradient is independent of the particular choice of tipping pulse (θ). Hence in each differential annulus Eq. (2) may be applied:

$$dm(r) = dm_0(r) \sin\theta \sin^2\theta e^{-2\pi T_2} \times \exp\{-\gamma^2 G^2 D \delta^2 [\tau - \frac{1}{3}\delta + A(2\tau/\delta - 1)]\} \quad (20)$$

and the induced signal is, by Eq. (19),

$$v(2\tau) \propto M(2\tau) \exp\{-\gamma^2 G^2 D \delta^2 [\tau - \frac{1}{3}\delta + A(2\tau/\delta - 1)]\}, \quad (21)$$

where $M(2\tau)$ represents a complex geometrical integral which is independent of G and δ and includes the T_2 dependence. Thus the functional dependence of the measured echo amplitude on pulsed gradient is exactly the same as in the case of an insulating sample.

Restricted-Medium Correction

The previous section had assumed that in the time over which diffusion is measured (τ), the spins translate over a distance much smaller than the skin depth. This assumption is partially violated for the concentrated lithium-ammonia solu-

tions. For the ^7Li resonance ($\tau = 25$ msec) in 20-MPM lithium ammonia at 240 K, the spins translate an rms distance of 0.15Δ along the z axis in 25 msec. Certainly some fraction of the spins will translate out of the skin depth into the interior of the sample in τ and will not contribute to the echo. However, since τ is held constant during a measurement, this reduction in echo amplitude may be absorbed into the definition of $M_0(2\tau)$ in Eq. (21).

A more serious complication is that the spins near the sample wall have a high probability of striking the wall in the time τ . If a large fraction of the spins were to collide with the wall, then the measured self-diffusion coefficient will be reduced from the "unrestricted" coefficient. Although restricted-medium corrections are known^{39,40} for simple geometries for insulating samples, no exact treatment of the corresponding problem in conductors is known. The magnitude of the restricted-medium correction for a cylindrical conductor may be estimated by treating the simpler case of an insulating liquid bounded by an annulus of radii R and $(R - \Delta)$, where $R \gg \Delta$. Since the pulsed gradients are applied in the z direction, only diffusion along z will reduce the echo amplitude. In Fig. 11 spins near $y = 0$ can move only Δ before striking a wall, whereas spins near $y = \pm R$ are less hindered. If the separation distance between walls measured along z is $L(y)$, then by weighting $L(y)$ by the spin density, the average spacing is

$$\langle L \rangle = (2/\pi) [1 - E(k) + (1 - k^2)K(k)], \quad (22)$$

where $k \equiv 1 - \Delta/R$ and $K(k)$ and $E(k)$ are complete elliptic integrals of the first and second kind, respectively. For $r = 2$ mm and $\Delta = 95 \mu$, then $\langle L(y) \rangle \approx 2\Delta$.

The effect of restricted diffusion for the annulus may then be further approximated by considering a planar geometry of spacing 2Δ . Robertson's expression³⁹ for the ratio of the restricted self-diffusion coefficient (D) to the unrestricted one (D_u) for the case of a planar geometry of spacing l and a steady field gradient may be modified for the pulsed-gradient case to yield

$$f' \equiv \frac{D}{D_u} = \frac{8\beta}{\alpha^2(1 - \frac{1}{3}\alpha)} \sum_{m=0}^{\infty} \frac{1}{\beta_m^4} \{ 2\alpha\beta_m - [2 + e^{-\beta_m(1-\alpha)} + e^{-\beta_m(1+\alpha)} - 2(e^{-\beta_m\alpha} + e^{-\beta_m})] \}, \quad (23)$$

where $\beta = D\tau/l^2$, $\beta_m = (2m+1)^2\pi^2\beta$, and $\alpha = \delta/\tau$. Here the pulses are assumed perfectly rectangular and background gradient effects are ignored. Figure 12 shows f' on calculating the first 50 terms in Eq. (23) for two representative values of α . Using Fig. 12 the correction term $(1 - f')$ is less than 8% for ^7Li in 20-MPM lithium ammonia at 240 K and less than 4% for the protons. In other samples

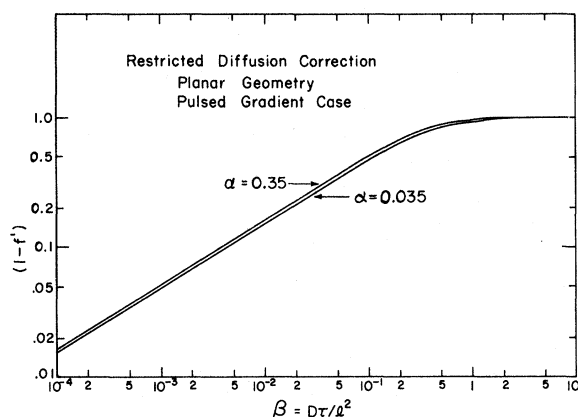


FIG. 12. Correction for restricted diffusion obtained from Eq. (23).

the corrections are correspondingly less.

As an actual test of the magnitude of the restricted-medium correction in a bulk-liquid conductor, the self-diffusion coefficient of ^7Li in molten lithium metal of natural isotopic abundance was measured at $189 \pm 1.5^\circ\text{C}$ and 18.5 MHz for $\tau = 25$ msec. The result is $D = (5.17 \pm 0.17) \times 10^{-5} \text{ cm}^2/\text{sec}$, where the quoted error represents only the statistical scatter. Murday^{13,41} has measured the self-diffusion coefficient of ^7Li in a dispersion of small

metal particles of natural isotopic abundance at melting. Extrapolating to 189°C , his result is $(6.4 \pm 0.8) \times 10^{-5} \text{ cm}^2/\text{sec}$. The error estimate excludes possible systematic error in the gradient-coil calibration since the same coil was used in his work and the present. His result includes a correction for the effects of a restricted medium in spherical conductors. Hence the measured self-diffusion coefficient in the bulk conductor is $(19 \pm 1.3)\%$ lower than Murday's value. The correction for restricted diffusion in the bulk conductor is estimated to be 13% by Fig. 12. Thus agreement is fair: The crude model employed in the derivation of Eq. (23) seems to be applicable. Since for the metal-ammonia solutions the effects of restricted diffusion are estimated to be not large and since diffusion data in the high-concentration regime are rather imprecise, no corrections for restricted diffusion were made to the metal-ammonia data.

It should be noted that the restricted-medium corrections in a bulk conductor may be reduced significantly by selecting a small value of τ ; e.g., for $\tau = 7$ msec, the correction for metallic lithium at melting is only 7%. Hence if one can tolerate a significant reduction in the signal-to-noise ratio, diffusion may be measured in bulk liquid metals by the pulsed-gradient spin-echo method, obviating the need to prepare dispersions of small particles.

*Work supported in part by the National Science Foundation through Grant No. GP-27531 and the Advanced Research Projects Agency through the Cornell Materials Science Center, Report No. 1874.

¹Present address: Department of Physics, University of Nottingham, Nottingham, NG7 2RD, England.

²M. H. Cohen and J. C. Thompson, *Adv. Phys.* **17**, 857 (1969).

³*Metal-Ammonia Solutions, Colloque Weyl I*, edited by G. Lepoutre and M. J. Sienko (Benjamin, New York, 1964).

⁴*Metal-Ammonia Solutions, Colloque Weyl II*, edited by J. J. Laboski and M. J. Sienko (Butterworths, London, 1970).

⁵J. A. Morgan, R. L. Schroeder, and J. C. Thompson, *J. Chem. Phys.* **43**, 4494 (1965).

⁶D. S. Kyser and J. C. Thompson, *J. Chem. Phys.* **43**, 3910 (1965).

⁷N. W. Ashcroft and G. Russakoff, *Phys. Rev. A* **1**, 39 (1970).

⁸R. L. Schroeder and J. C. Thompson, *Phys. Rev.* **179**, 124 (1969).

⁹J. C. Thompson, *Phys. Rev. A* **4**, 802 (1971).

¹⁰N. Mammano and M. J. Sienko, *J. Am. Chem. Soc.* **90**, 6322 (1968).

¹¹A. Demortier, P. Labry, and G. Lepoutre, *J. Chim. Phys.* **68**, 498 (1971).

¹²R. H. Maybury and L. V. Coulter, *J. Chem. Phys.* **19**, 1326 (1951).

¹³E. D. Stejskal and J. E. Tanner, *J. Chem. Phys.* **42**, 288 (1965).

¹⁴J. S. Murday, Ph.D. thesis (Cornell University, 1970) (unpublished).

¹⁵G. W. Castellan, *Physical Chemistry* (Addison-Wesley, Reading, Mass., 1964), p. 42.

¹⁶J. H. Simpson and H. Y. Carr, *Phys. Rev.* **111**, 1201 (1958).

¹⁷H. R. Pruppacher, *J. Chem. Phys.* **56**, 101 (1972).

¹⁸D. E. O'Reilly, E. M. Peterson, and S. R. Lammert, *J. Chem. Phys.* **52**, 1700 (1970).

¹⁹J. G. Powles, M. Rhodes, and J. H. Strange, *Mol. Phys.* **11**, 515 (1966).

²⁰R. A. Ogg and J. D. Ray, *J. Chem. Phys.* **36**, 1515 (1957).

²¹J. Frenkel, *Kinetic Theory of Liquids* (Dover, New York, 1955), p. 192.

²²*Handbook of Chemistry and Physics*, 41st ed., edited by C. D. Hodgman (Chemical Rubber, Cleveland, Ohio, 1959).

²³T. Nozaki and M. Shimoji, *Trans. Faraday Soc.* **65**, 1489 (1969).

²⁴D. W. McCall and D. C. Douglass, *J. Chem. Phys.* **69**, 2001 (1965).

²⁵P. Ascarelli and A. Paskin, *Phys. Rev.* **165**, 222 (1967).

²⁶C. J. Vadovic and C. P. Colver, *Phys. Rev. B* **1**, 4850 (1970).

²⁷C. J. Vadovic and C. P. Colver, *Philos. Mag.* **21**, 971 (1970).

²⁸C. J. Vadovic and C. P. Colver, *Philos. Mag.* **24**, 509 (1971).

²⁹N. Carnahan and K. Starling, *J. Chem. Phys.* **51**, 635 (1965).

³⁰N. W. Ashcroft and J. Lekner, *Phys. Rev.* **145**, 83 (1966).

³¹R. E. Lo, *Z. Anorg. Allgem. Chem.* **344**, 240 (1966).

³²N. W. Ashcroft and D. C. Langreth, *Phys. Rev.* **159**, 500 (1967).

³³D. E. Bowen, J. C. Thompson, and W. E. Millett, *Phys. Rev.* **168**, 114 (1968).

³⁴M. H. Cohen and C. Turnbull, *J. Chem. Phys.* **31**, 1164 (1959).

³⁵A. Ott and A. Lodding, *Z. Naturforsch. A* **20**, 1578 (1965).

³⁶H. J. Saxton and O. D. Sherby, *ASM Trans. Q. (Am. Soc. Met.)* **55**, 826 (1962).

³⁷A. K. Saha and T. P. Das, *Theory and Applications of Nuclear Induction* (Saha Institute of Nuclear Physics, Calcutta, 1957),

p. 45.

³⁷L. A. McLachlan, Ph.D. thesis (University of British Columbia, 1965) (unpublished).

³⁸B. Muller and M. Bloom, *Can. J. Phys.* **38**, 1318 (1960).

³⁹B. Robertson, *Phys. Rev.* **151**, 273 (1966).

⁴⁰C. H. Neuman (private communication).

⁴¹J. S. Murday and R. M. Cotts, *Z. Naturforsch. A* **26**, 85 (1971).

PHYSICAL REVIEW A

VOLUME 7, NUMBER 2

FEBRUARY 1973

Uniform WKB Theory of Inelastic Collisions: Application to He⁺-Ne Inelastic Collisions*

Byung Chan Eu[†] and Thomas P. Tsien

Department of Chemistry, McGill University, Montreal, Canada

(Received 18 September 1972)

The uniform WKB theory of inelastic collisions is discussed further and applied to a semi-classical analysis of the He⁺-Ne inelastic collisions [$\text{He}^+ + \text{Ne}(2p^6) \rightarrow \text{He}^+ + \text{Ne}^*(2p^53s)$] at $E=70.9$ eV. The uniform WKB differential cross section of the inelastic scattering is compared with that of the Landau-Zener-Stückelberg theory of inelastic collisions. The result of comparisons indicates that the uniform WKB theory is more reliable than the Landau-Zener-Stückelberg theory and the distorted-wave-Born-approximation theory.

I. INTRODUCTION

There has been an enormous amount of experimental data accumulated on inelastic scattering of atomic and molecular systems which await theoretical analysis. Occasionally it is possible in practice to attempt a completely numerical analysis for some systems, but such an attempt is impractical and costly for most cases experimentally investigated so far. We are therefore compelled to resort to approximate theories like the distorted-wave Born approximation¹ (DWBA), the Landau-Zener-Stückelberg (LZS) theory,² and other semiclassical theories,^{3,4,5(c)} to cite a few. The LZS theory has been very useful for some inelastic-scattering problems like electronic excitations of atomic systems, molecular internal excitations, and molecular dissociations, when such processes involve a potential curve crossing. However, the LZS theory has a limited capability,⁵ since it cannot predict correct transition probabilities as the coupling between two different channels increases,⁶ and is not applicable at all if there is no curve-crossing point: The theory simply predicts zero transition probabilities, for example, if the two potential curves are parallel. This is in contrast with what we find from the numerical solution of the same problem.

Olson and Smith⁷ compared the LZS theory with the DWBA in their recent paper on the analysis of He⁺-Ne inelastic collision processes and found that the former was not comparable to the latter as far as the angular distribution of the inelastic scattering was concerned.

Recently, one of us has developed a semiclassical (uniform WKB) theory⁴ of inelastic scattering that has no defects of the LZS theory and, thus, can

deal with the cases of a large coupling parameter⁶ both with and without a curve crossing. The theory has been shown^{4(c)} to reduce essentially to the Landau-Zener theory as the coupling constant decreases to zero. It is one of the purposes of the present paper to apply the uniform WKB (UWKB) theory to a practical problem to show the utility of the theory. In this paper we also wish to clarify further some of the details which have not been discussed yet, but are necessary for practical application of the theory. We choose as an example He⁺-Ne inelastic scattering^{7,8} which may be adequately described by a two-channel approximation. In order to exhibit the capability of the theory, we also compare the differential cross section of the UWKB theory with those of the LZS theory and the DWBA.

In Sec. II we briefly review the UWKB theory to define notations and to make feasible a discussion on the practical use of the theory and some of the details which have not been discussed before. In Sec. III we apply the theory to an analysis of the He⁺-Ne system and compare it with the LZS theory and the DWBA. The result of calculations shows that the UWKB theory is more reliable. In Sec. IV we discuss the LZS theory further and discuss the necessity of retaining more channels than two for a more realistic and accurate analysis of the He⁺-Ne inelastic process. Some differences between the present theory and the Thorson-Delos-Boorstein theory^{5(c)} are also discussed.

II. UWKB THEORY

In this section we shall first briefly review the UWKB theory^{4(c),4(d)} and then discuss computations of the approximate S-matrix elements. In the UWKB theory the solution of coupled radial Schrö-